*Int. J. Electrochem. Sci.*, 8 **(2013)** 1295 - 1307

**International Journal of**
**ELECTROCHEMICAL**
**SCIENCE**
www.electrochemsci.org

# Experimental Investigation and Theoretical Approach on Water Soluble Rosin as Corrosion Inhibitors

*Ayman M Atta*[1, 2], *Gamal A El-Mahdy*[1,3 *], *Adel A. Al-Azhary*[1] *and Hamad A. Al-Lohedan*[1]

[1] Chemistry Department, College of Science, King Saud University, Riyadh 11541, Saudi Arabia
[2] Petroleum Applications Department, Egyptian Petroleum Research Institute (EPRI), Naser City 11727, Cairo, Egypt.
[3] Chemistry Department, Faculty of Science, Helwan University, Cairo, Egypt
[*]E-mail: Gamalmah2000@yahoo.com

*Received:* 5 November 2012 / *Accepted:* 11 December 2012 / *Published:* 1 January 2013

---

Rosin poly(oxyethylene) ester 4,5-dihydroimidazole maleate Adduct (RIMA-PEG), has been applied as corrosion inhibitor for carbon steel. Experimental data for the inhibition efficiency using potentiodynamic polarization, electrochemical impedance spectroscopy (EIS) technique and theoretical quantum chemical calculations data indicated that their inhibition effect are closely related to $E_{HOMO}$, $E_{LUMO}$, hardness, dipole moment and charge densities. A mechanism for adsorption of RIMA-PEG molecules on carbon steel surface is suggested.

---

**Keywords:** Acid inhibitor, Carbon steel, EIS, Polarization, Quantum chemical calculations

## 1. INTRODUCTION

The inhibition of steel in acid solutions by different types of organic inhibitors has been extensively studied [1–7]. Most of organic substance employed as corrosion inhibitors can adsorb on the metal surface through hetero-atoms such as nitrogen, oxygen, sulfur, phosphorus, multiple bonds or aromatic rings and block the active sites, decreasing the corrosion rate [8–12]. The intrinsic ability of surfactant molecules to easily adsorb on surfaces and interfaces is associated with their amphiphilic structure. They form a protecting interfacial film against the action of corrosion agents in solid–liquid systems [13]. The adsorption of surfactants on surfaces depends on the structure and concentration of surfactant molecules in the contacting medium, determining the final adsorption layout with the formation of monolayers or multilayers of surfactant molecules [14]. Many researchers currently focusing in synthesis of new materials from renewable natural resources to replace environmentally and energy unfavorable plastics derived from petroleum chemicals [15-17]. Water-soluble synthetic polymers have been prepared and used as surface active agents owing to their amphipathic structure and surface activity. Nonionic surfactants were prepared in our previous work, from rosin acid and used as flow improver and oil spill dispersant for petroleum crude oil [18-20]. Recently, the structure of the rosin was confirmed by Fourier transform infrared (FTIR) and was used as a new class of inhibitor for carbon steel [21]. It has been observed that the adsorption depends mainly on the electronic and structural properties of the inhibitor molecule such as functional groups, steric factors, aromaticity, electron density on donor atoms and π orbital character of donating electrons [22–28]. The geometry of the inhibitor in its ground state, as well as the nature of their molecular orbitals, HOMO (highest occupied molecular orbital) and LUMO (lowest unoccupied molecular orbital) are involved in the properties of inhibitors activity. Quantum chemistry calculations have been widely used to study the reaction mechanisms and to interpret the experimental results [29–32]. The structure and electronic parameters can be obtained by means of theoretical calculation using the computational methodologies of quantum chemistry [33-34]. Quantum Chemical calculations have become an effective method to study the correlation of the molecular structure and its inhibition properties [35-39].

In this work, non-toxic modified rosin hydroimidazole have been Synthesized from rosin acid adducts and applied as corrosion inhibitors for carbon steel. The investigation is performed using electrochemical methods as well as electrochemical impedance spectroscopy (EIS) measurements. The work will extend to find a correlation between the inhibition efficiency and the electronic properties of the studied molecules. A mechanism for adsorption of rosin molecules on carbon steel surface is suggested

## 2. EXPERIMENTAL

### *2.1. Materials*

Rosin were heated at 150$^o$C for 4 hours then heated at 200$^o$C for 30 minutes in nitrogen atmosphere to isomerizes rosin acids to leveopimaric acid, then it were separated by crystallization from the cold acetone solution of commercial rosin. Rosin acids with acid number 183mg KOH.g$^{-1}$ and melting point 167$^o$C was obtained from commercial rosin [20]. The separation of the rosin acids from rosin was carried out to increase the yield and to remove terpens, which have the ability to react with maleic anhydride. Maleic anhydride (MA), ethylene diamine (EDA), p-toluene sulfonic acid (PTSA), poly (ethylene glycol), PEG, having molecular weights 400 and 600 designated as PEG 400 and PEG 600 were supplied from Aldrich Chemicals Co. (USA) and used as received. 1M HCl was prepared by appropriate dilution of analytical grade HCl with double distilled water and used as test solution. .

Corrosion tests were performed on a carbon steel sheet having the following chemical composition (wt %): 0.3% C, 0.02% Si, 0.03% Mn, 0.045% Sn, 0.04% P and the remainder Fe. A carbon steel disc of the same chemical composition was mounted in Teflon with an exposed surface area of 1 cm$^2$ was used as working electrode. The electrode was mechanically polished with different grades of silicon carbide papers, degreased in ethanol to obtain a fresh oxide-free surface, washed with bi-distilled water and dried at room temperature.

### *2.1.2Quantum Chemical Calculations*

All the quantum calculations were performed with complete geometry optimization by using standard Gaussian09 software [40].

## *2.2 Procedure*

### *2.2.3 Preparation of rosin poly(oxyethylene) ester 4,5-dihydroimidazole maleate Adduct (RIMA-PEG)*

A mixture of freshly distilled PEG 400 or PEG 600 (1.1 mol), RIMA (1 mol), PTSA (1%) based on total weight of reactants and 100 ml xylene were placed in 0.5 L round-flask fitted with Dean Stark apparatus. The mixture was allowed to reflux until the theoretical water was collected. Xylene was distilled off from the reaction product by rotary evaporator under reduced pressure. The product was separated by salting out use saturated NaCl solution and extracted with isopropanol using separating funnel. The purified products were isolated after evaporation of isopropanol. . Details about the methods of preparation and the identification of chemical structure of the prepared RIMA-PEG were completely described in our previous work [21].

## *2.3 Measurements*

Electrochemical tests were conducted using Volta lab 40 (Tacussel-Radiometer PGZ301) potentiostat controlled by Tacussel corrosion analysis software model (Voltamaster 4). All the measurements were performed using a three-electrode system arrangement, with carbon steel as the working electrode A platinum electrode and a saturated calomel electrode (SCE) were used as the reference and counter electrode, respectively. The working electrode was prepared from a cylindrical carbon steel rod insulated with polytetrafloroethylene tape (PTFE). The area exposed to the aggressive solution was $1 cm^2$. Impedance measurements were performed using Tacussel-Radiometer PGZ 301 Frequency Response Analyzer in a frequency range from $10^5$ to $10^{-2}$ Hz with 10 points per decade. An AC sinusoid ±10mV was applied at the corrosion potential ($E_{corr}$).

# 3. RESULTS AND DISCUSSION

## *3.1 Effect of temperature*

The effect of temperature on the inhibition efficiency of RIMA-PEG 600 inhibitor at 600 ppm concentration was determined at temperatures range of 25, 35, 45 and 55 $^{o}$C using potentiodynamic polarization curves. The results are displayed in Fig. 1. The corresponding data estimated from the polarization curves are given in Table 1.

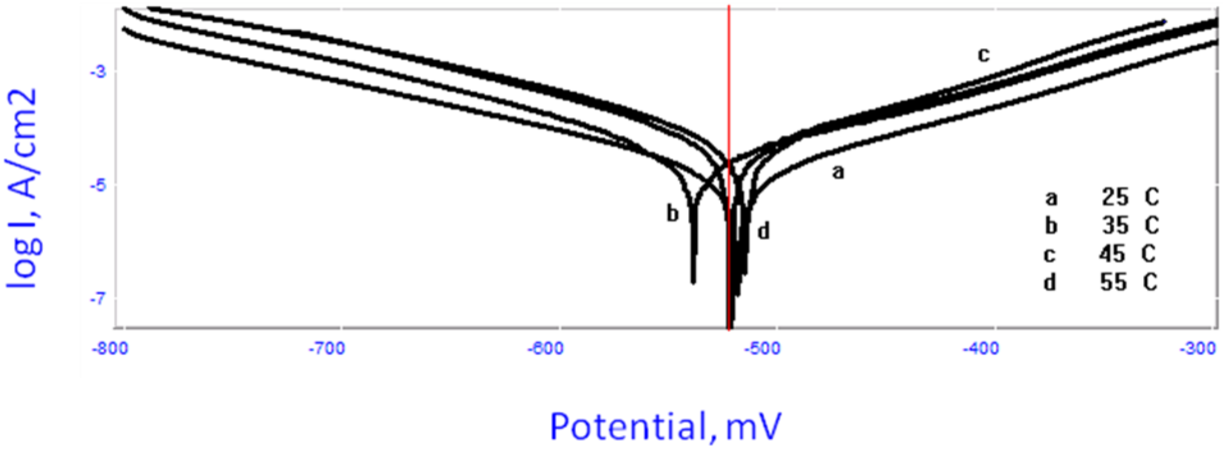

**Figure 1.** Effect of temperature on the cathodic and anodic polarization for carbon steel in 1 M HCl with 250 ppm of RIMA-PEG 600 inhibitors.

**Table 1.** Effect of temperature on the electrochemical parameters for carbon steel electrode immersed in 1 M HCl in the presence of 250 ppm of RIMA-PEG600 inhibitor.

| Temperature (°C) | $-E_{corr}$, mV | $I_{corr}$, $mA/Cm^2$ | $R_P$, $\Omega Cm^2$ | $\beta_a$, $mV/dec^{-1}$ | $\beta_c$, $mV/dec^{-1}$ | C.R mmy | I% |
|---|---|---|---|---|---|---|---|
| 25 | 517 | 0.02 | 2470 | 98.9 | 120 | 0.240 | 97.15 |
| 35 | 537 | 0.06 | 514.84 | 112.0 | 117 | 0.717 | 97.6 |
| 45 | 521 | 0.089 | 444.7 | 101.5 | 113.6 | 1.041 | 98.28 |
| 55 | -514 | 0.107 | 144.57 | 110.3 | 125.2 | 1.253 | 98.61 |

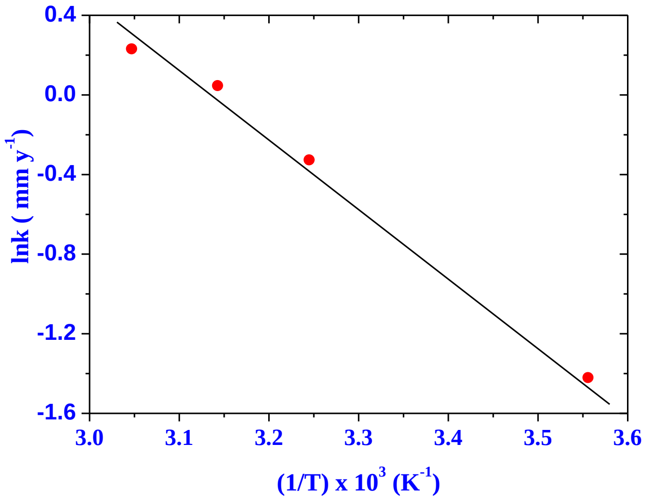

**Figure 2.** Arrhenius plot of carbon steel immersed in 1 M HCl solution.

The dependence of inhibition efficiency on temperature is shown in Fig. 2. The data shows that the inhibition efficiency of RIMA-PEG 600 increases with increasing temperature. The increase of inhibition efficiency and its dependence on temperature suggests that a chemi-sorptive bond between the RIM-PEG molecules and the iron surface is probable. It can be concluded that the inhibitor has experienced a significant increase in its degree of protectiveness with increasing temperature. The data can be explained on the basis of flat mode of adsorption of RIMA-PEG 600 molecules, which in turn covers a large area of the exposed surface and hence, inhibiting effectively the corrosion process. This suggests that the adsorbed layer covers quickly the entire surface and simultaneously blocks the active site of corrosion on the surface. A similarity in results has been reported elsewhere for increasing the inhibition efficiency with increasing temperature [41-46]. It has been reported previously by a number of authors that the logarithm of the corrosion rate of steel in acid solution is a linear function with 1/T following Arrhenius equation [47-51]:

$$\ln k = - E_a / RT + \ln A \qquad (1)$$

where, k is the corrosion rate, $E_a$ is the apparent activation energy of the corrosion reaction, R is the gas constant, T is the absolute temperature and A is a frequency factor. Fig. 2 represents the Arrhenius plots (ln k vs. 1/T) of carbon steel corrosion in 1M HCl solution. The activation energy (Ea) was calculated and found to be 18.93 kJ $mol^{-1}$.

### *3.2 EIS measurements*

The effects of RIMA-PEG inhibitors at different concentrations on the impedance behavior of iron in 1 M HCl solutions are shown in Figs. 3 and 4.

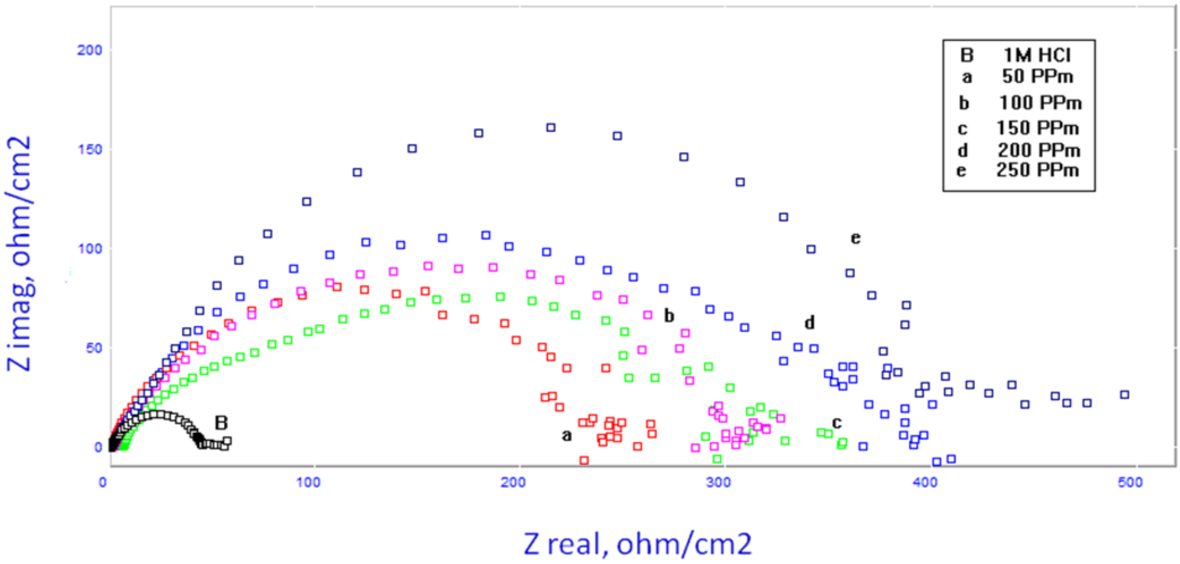

**Figure 3.** Nyquist plots for carbon steel immersed in 1M HCl solution in the absence and presence of various concentrations of RIMA-PEG 400 inhibitor.

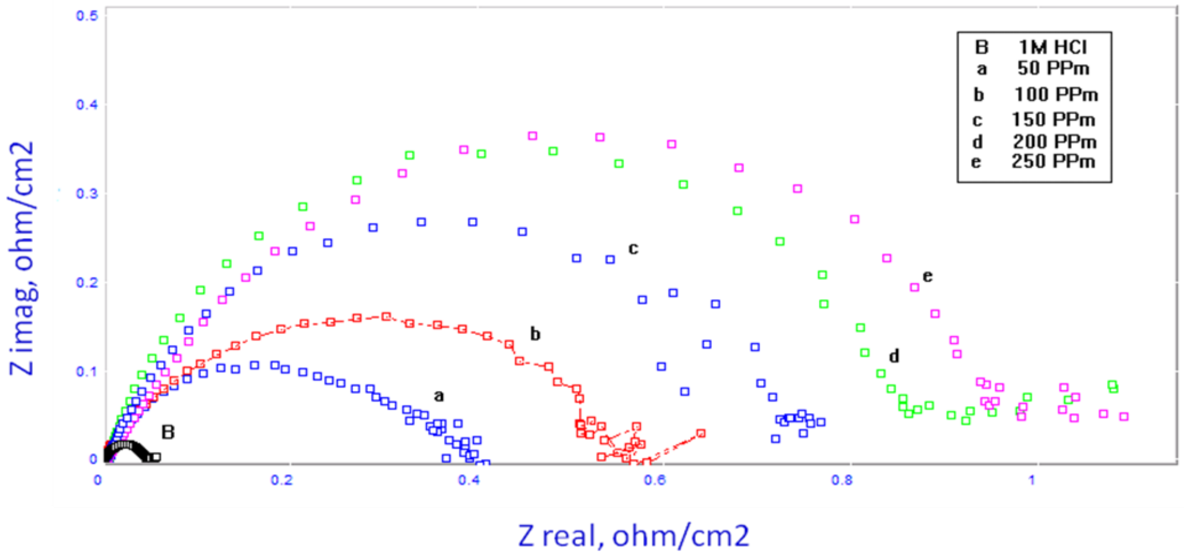

**Figure 4.** Nyquist plots for carbon steel immersed in 1M HCl solution in the absence and presence of various concentrations of RIMA-PEG 600 inhibitor.

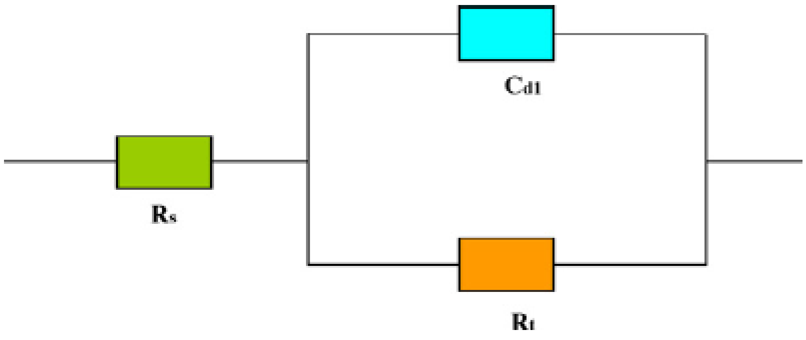

**Figure 5.** The equivalent circuit model for the electrochemical impedance measurements.

It is clear from Nyquist plots (Figs. 3-4) recorded for carbon steel electrode immersed in 1M hydrochloric acid solution at 25 ◦C in absence and presence of various concentrations of the RIMA-PEG inhibitors that imperfect semicircles were obtained. This behavior can be attributed to frequency dispersion [52]. For analysis of the impedance spectra contain one capacitive loop, a simple equivalent circuit consisting of a parallel combination of a capacitor, $C_{dl}$, and a resistor, $R_t$, in series with a resistor, $R_s$, representing the solution resistance. The proposed equivalent circuit is shown in Figure 5. The electrode impedance, Z, in this case is represented by the mathematical formulation [53]:

$$Z = Rs + [\ (R_t)/1+(2\pi f R_t C_{dl})^{\alpha}] \qquad (2)$$

where α denotes an empirical parameter ($0 \leq \alpha \leq 1$) and f is the frequency in Hz. Eq. (2) takes into account the deviation from the ideal RC-behavior in terms of a distribution of time constant due to surface heterogeneity, roughness effects, adsorption of inhibitors and variations in properties or compositions of surface layers. Various electrochemical parameters derived from Nyquist plots are calculated and listed in Tables 2-3.

**Table 2.** Data from electrochemical impedance spectroscopy measurements of carbon steel in 1MHCl solution in the absence and presence of vrious concentrations of RIMA-PEG 400 inhibitor.

| Conc. (ppm) | $R_s$ (ohm cm$^2$) | $R_t$ (ohm cm$^2$) | $C_{dl}$ (µF cm$^{-2}$) | I% |
|---|---|---|---|---|
| 0 | 1.522 | 49.28 | 1020 | |
| 50 | 1.754 | 246 | 0.102 | 79.9 |
| 100 | 3.13 | 308.9 | 0.081 | 84 |
| 150 | 6.8 | 320.8 | 0.1 | 85.01 |
| 200 | 2.04 | 387.2 | 0.025 | 87.27 |
| 250 | 3.24 | 438.8 | 0.145 | 88.7 |

**Table 3.** Data from electrochemical impedance spectroscopy measurements of carbon steel in 1MHCl solution in the absence and presence of various concentrations of RIMA-PEG 600 inhibitor.

| Conc. (ppm) | $R_s$ (ohm cm2) | $R_t$ (ohm cm$^2$) | $C_{dl}$ (µF cm$^{-2}$) | I% |
|---|---|---|---|---|
| 0 | 1.522 | 49.28 | 1020 | d |
| 50 | 87.2 | 387.2 | 44.35 | 87.2 |
| 100 | 91.3 | 566.9 | 25.97 | 91.3 |
| 150 | 93.39 | 746.2 | 0.106 | 93.39 |
| 200 | 94.82 | 952.8 | 0.66 | 94.82 |
| 250 | 95.07 | 1017 | 0.078 | 95.07 |

The values of $R_t$ were given by subtracting the high frequency impedance from the low frequency one as follows [54]:

$$R_t = Z\ (\text{at low frequency}) - Z\ (\text{at high frequency}) \qquad (3)$$

The values of electrochemical double layer capacitance $C_{dl}$ were calculated at the frequency $f_{max}$, at which the imaginary component of the impedance is maximal ($-Z_{max}$) by the following equation [55]:

$$C_{dl} = [1/2\pi f_{max}]\ [1/\ R_t] \qquad (4)$$

The values of percentage inhibition efficiency( I%) were calculated from the values of $R_t$ according to the following equation [56]:

$$IE\% = (R_{t(inh.)} – Rt)/R_{t(inh.)} \quad (5)$$

Where $R_t$ and $R_{t(inh.)}$ are the values of the charge transfer resistance in the absence and presence of the inhibitor, respectively. The impedance data listed in Tables 2-3 indicate that the values of both $R_t$ and I% are found to increase by increasing the inhibitor concentration, while the values of $C_{dl}$ are found to decrease. This behavior can be attributed to a decrease in dielectric constant and/or an increase in the thickness of the electrical double layer, suggesting that the inhibitor molecules act by adsorption mechanism at carbon steel/acid interface [57]. The data obtained from EIS are in good agreement with that obtained from potentiodynamic polarization.

### *3.3 Quantum Chemical Calculations*

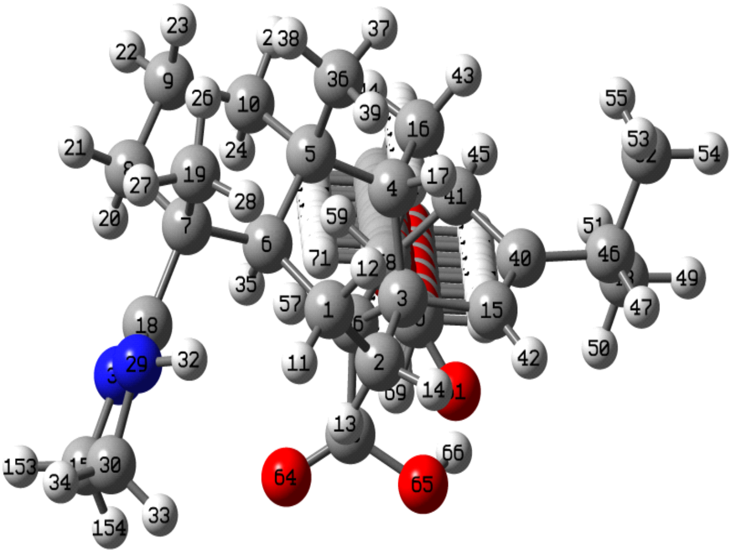

**Figure 6.** Structure of RIMA-PEG 600.

Electric charges in the molecule are obviously responsible for electrostatic interactions. The distribution of the charges is important in many chemical reactions and for physico-chemical properties of compounds. Thus, charge-based parameters have been widely employed as chemical reactivity indices. The charge distribution in a molecule was calculated by standard Gaussian09 software [40] depending upon Mulliken population analysis [58], which provides a qualitative understanding of the structure and reactivity of molecules [59]. The charge density of the atoms was calculated for RIMA-PEG molecule with n= 12 and 9. It was found that the highest electronegative atom is nitrogen atom number 29, which is considered as the most reactive center for adsorption. Fig. 6 shows the structure of RIMA-PEG 600. It was reported previously that the atom which had the more negative atomic charges had the ability to donate easily its electron to the unoccupied orbital of metals [60]. The molecular orbital, HOMO (highest occupied molecular orbital), LUMO (lowest unoccupied molecular orbital) and dipole moment $\mu$ (D) total energy are calculated and presented in Table 4. HOMO orbital acts as an electron donor, since it is the outermost (highest energy) orbital containing electrons. The energy of the HOMO is directly related to the ionization potential and the energy of the LUMO is directly related to the electron affinity. The HOMO–LUMO gap, i.e. the difference in energy between the HOMO and LUMO, is an important stability index [61]. A large HOMO–LUMO gap implies high stability for the molecule in chemical reactions [62].

**Table 4.** The calculated quantum chemical properties for RIMA-PEG molecules

| Quantum Chemical parameters | n =9 | n=12 |
|---|---|---|
| $E_{\mathrm{HUMO}}$ (eV) | -0.33348 | -0.33350 |
| $E_{\mathrm{LUMO}}$ (eV) | 0.16353 | 0.16351 |
| $\eta$ (eV) | 0.248505 | 0.248505 |
| Dipole moment (D) | 7.3657 | 5.8574 |

The energy gap between HOMO and LUMO is small and indicating a higher electron donating ability of the inhibitor to the metallic surface. According to molecular orbital theory the hardness of the molecules can be calculated from the following equation [63]:

$$\eta = (\varepsilon_{\mathrm{LUMO}} - \varepsilon_{\mathrm{HUMO}})/2 \qquad (8)$$

A soft molecule has a small energy gap and is more reactive than a hard molecule with a large energy gap. RIMA-PEG molecule has a small energy gap as shown in table 4 indicating the softness of the molecule (soft-soft interaction)

The high efficiency of the RIMA-PEG molecule may be attributed to the high value of HOMO energy of the inhibitor, which facilitates the susceptibility of the molecule to donate electron to the unoccupied orbital of the metal. In addition, the small value of HUMO–LUMO energy gap reinforces the adsorption of the inhibitor on the metallic surface due to a strong columbic interaction. The most widely used quantity to describe the polarity is the dipole moment of the molecule [64]. It is defined as the product of charge on the atoms and the distance between the two bonded atoms. The total dipole moment reflects only the polarity of a molecule and may be approximated as the vector sum of individual bond dipole moments. The efficiency of the inhibitor increases with lower dipole moments [65-66]. RIMA-PEG molecule with n=12 has a lower value of dipole moments than RIMA-PEG molecule with n=9 (Table 4), which give an evidence for the higher efficiency of RIMA-PEG molecule with n=12

### *3.4 Mechanism of inhibition*

Many mechanisms have been proposed for the inhibition of metal corrosion by organic inhibitors. Generally, it has been assumed that the first stage in the action mechanism of the inhibitor in the aggressive acid media is based on its adsorption on the metal surface [67]. The processes of adsorption of inhibitors are influenced by the nature of the metal surface, the chemical structure of the organic inhibitor, the distribution of charge in the molecule, the type of aggressive electrolyte, and the type of interaction between organic molecules and the metallic surface [68-69].

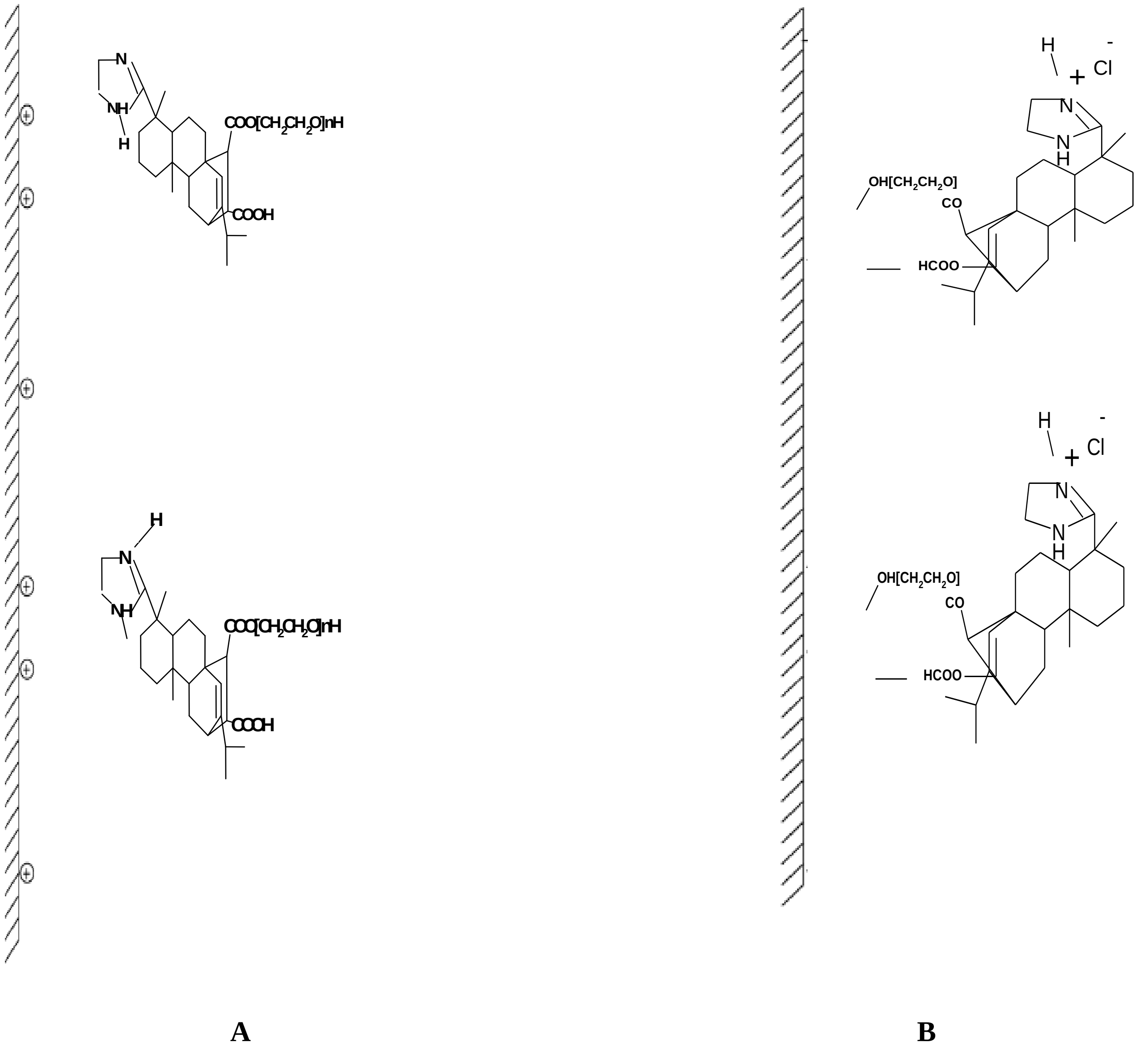

**Figure 7.** Schematic representation of adsorption behavior of RIMA-PEG on mild steel in 1 MHCl solution: (a) mild steel surface with positive charge, (b) Adsorption on mild steel surface through oxyethylene group of RIMA-PEG

In most inhibition studies, the formation of donor-acceptor surface complexes between p-electrons of an inhibitor and the vacant d-orbital of metal were postulated [70]. Nitrogen-based compounds are effective inhibitors for mild steel corrosion in aqueous solutions [71]. The presence of lone pairs of electrons on the nitrogen atoms of the additional nitrogen atoms delocalised and thus produced a delocalization energy that stabilised the compound. It is also known that the adsorption of the inhibitor can be influenced by the nature of the anions in acidic solution. The presence of $Cl^-$ in the solution should be mentioned. They are characterized with strong adsorbability on the metal surface which brings about a negative charge favoring the adsorption of cation type inhibitors [72].

The RIMA-PEG consisting of a five-member ring (imidazole) combined with hydrophenancere ring. It has two nitrogen atoms, which have unshared electron pair remains free and facilitates the reaction with acids to give salts. RIMA-PEG are organic bases but the presence of an imine (–NH) group in the molecule determines well-outlined acidic properties as well. This means that the addition of an acid or a base to the aqueous solution of this compound will transform the neutral molecule into a cation or an anion [73]. The performance of RIMA-PEG in HCl can be explained on the basis of the calculated charge density of atoms. It is well known that the more negative the atomic charges of the adsorbed centre, the more easily of the atom to donate its electrons to the unoccupied orbital of metal [61]. Nitrogen atom with number 29 has the highest charge density and becomes the active adsorption center. A schematic representation of the adsorption behavior of RIMA-PEG on mild steel in 1 M HCl solution is shown in Fig. 7 (a-b). The RIMA-PEG molecule will be adsorbed on the positively charged metal surface through the nitrogen atom number 29 (Fig. 7a). Thus, a close packed triple layer will form on the metal surface and inhibit the entry of iron ions to the solution. Hence, with an increase in the positive charge on the metal surface, the adsorption of RIMA-PEG would increase and the RIMA-PEG content in the solution would decrease. The strong inhibition efficiency of RIMA-PEG molecule was attributed to the small value of HUMO–LUMO energy gap, dipole moment and the hardness of the molecules ($\eta$), which reinforces the adsorption of the inhibitor on the metallic surface due to a strong columbic interaction. A few RIMA-PEG molecules may, however, become adsorbed through their oxyethylene group of PEG on the metal surface (which possesses vacant d$\pi$-orbitals (Fig. 7b). The formation of such protective film was confirmed by electrochemical impedance spectroscopy (EIS). The calculated high inhibition efficiency (I %) can be attributed to strong adsorption ability of RIMA-PEG molecules on carbon steel surface.

## 4. CONCLUSIONS

The main conclusions of the present study are summarized in the following points:

1- RIMA-PEG can be used with an excellent efficiency for corrosion inhibition of carbon steel in 1M HCl solution,

2- The strong inhibitive effect of RIMA-PEG can be attributed to the small value of HUMO–LUMO energy gap, dipole moment and the hardness of the molecules ($\eta$), which in turn reinforces the adsorption of the RIMA-PEG on the metallic surface.

3-The inhibition efficiency of the water soluble rosin as corrosion inhibitors indicates that their inhibition effect are closely related to EHOMO, ELUMO, hardness, dipole moment and charge densities.

4- A mechanism for adsorption of RIMA-PEG molecules on carbon steel surface is suggested.

ACKNOWLEDGMENT

The authors extend their appreciation to the Deanship of Scientific Research at King Saud University for funding the work through the research group Project No. RGP-VPP-148.

## References

1. F. Zucchi, G. Trabanelli, G. Brunoro, *Corros. Sci.* 36 (1994) 1683.
2. J.M. Bastidas, J.L. Polo, E. Cano, *J. Appl. Electrochem*. 30 (2000) 1173.
3. P.K. Ghosh, D.K. Guhasarkar, V.S. Gupta, *Br. Corros. J.* 18 (1983) 187.
4. E.E. Foad El Sherbini, *Mater. Chem. Phys*. 60 (1999) 286.
5. W.W. Frenier, F.B. Growcock, V.R. Lopp, *Corrosion* 44 (1988) 590.
6. M.A. Quraishi, D. Jamal, *Corrosion* 56 (2000) 156.
7. V.S. Sastri, Corrosion Inhibitors—Principles and Applications, Wiley,
Chichester, England, 1998.
8. G. Benerjee, S.N. Malhotra, *Corrosion* 48 (1992) 10.
9. A. El-Sayed, *J. Appl. Electrochem*. 27 (1997) 193.
10. S. Rengamani, S. Muralidharan, M. Anbu Kulandainathan, S. VenkatakrishnaIyer, *J. Appl. Electrochem.* 24 (1994) 355.
11. R. Agrwal, T.K.G. Namboodhiri, *J. Appl. Electrochem.* 22 (1992) 383.
12. C. Fiaud, A. Harch, D. Mallouh, M. Tzinmann, *Corros. Sci.* 35 (1993)1437.
13. R. Atkin, V.S.J. Craig, E.J. Wanless, S. Biggs, *Adv. Coll. Int. Sci.* 103 (2003) 219.
14. Y. Reyes, F.J. Rodfguez, J.M. del Rio, M. Corea, F. Vazquez, *Prog. Org. Coatings* 52 (2005) 366.
15. C. K. Williams, M. A. Hillmyer, *Polym. Rev. 48* (2008) 1.
16. 16. A. I. Corma, A. S. Velty, *Chem. Rev. 107* (2007) 2411.
17. D. R. Dodds, R. A. Gross, *Science*, *318*( 2007)1250.
18. A. M. Atta, A. M. Ramadan, K. A. Shaffei, A. M. Nassar, N. S. Ahmed, M. Fekry, *J. Disper. Sci. Technol*, 30 ( 2009) 1100.
19. A.M. Al-Sabagh, T.T. Khidr, , A.M. Atta, *Pet. Sci. Technol*., 20 (2002) 693.
20. A. M. Atta, M. E. Abdel-Rauf, N.E. Maysour, A. K. Gafer, *J. Disper. Sci. Technol* 31 (2010)583.
21. A. M. Atta, G. A. EL-Mahdy and H. A. Al-lohedan, accepted for publication in *Inter. J. Electrochem. Sci*., 7 (2012).
22. E. Khamis, *Corrosion* 46 (1990) 476.
23. E. Stupnisek-Lisac, S. Podbrscek, *J. Appl. Electrochem.* 24 (1994) 779.
24. E. Stupnisek-Lisac, M. Metikos-Hukovic, *Br. Corros. J.* 28 (1993) 74.
25. S.L. Granese, B.M. Rosales, C. Oviedo, J.O. Zerbino, *Corros. Sci.* 33 (1992) 1439.
26. S.L. Granese, *Corrosion* 44 (1988) 322.
27. M.A. Quraishi, H.K. Sharma, *Chem. Phys.* 78 (2002) 18.
28. M.A. Quraishi, R. Sardar, *Mater. Chem. Phys.* 78 (2002) 425.
29. F.B. Growcock, *Corrosion* 45 (1989) 1003.
30. I. Lukovits, K. Pa´lfi, I. Bako´, E. Ka´lma´n, *Corrosion* 53 (1997) 915.
31. I. Lukovits, A. Shaban, E. Ka´lma´n, *Russ. J. Electrochem*. (2003) 177.
32. F. Bentiss, M. Lagrene´e, M. Traisnel, H. Vezin, *Corros. Sci.* 45 (2003) 371.
33. F. Kandemirli, S. Sagdinc, *Corros. Sci.* 49 (2007) 2118.
34. D. Wang, S. Li, Y. Ying, M. Wang, H. Xiao, Z. Chen, *Corros. Sci.* 41 (1999) 1911.
35. S.L. Li, Y.G.Wang, S.H. Chen, R. Yu, S.B. Lei, H.Y. Ma, D.X. Liu, *Corros. Sci.* 41 (1999) 1769.
36. L. Mar´ıa Rodr´ıguez-Valdez, A. Mart´ınez-Villafa˜ne, D. Glossman-Mitnik, *J. Mol. Struct.* 713 (2005) 65.
37. F. Bentiss, M. Lagren´ee, B. Elmehdi, B. Mernari, M. Traisnel, H. Vezin, *Corrosion* 58 (2002) 399.
38. V.S. Sastri, J.R. Perumareddi, *Corrosion* 53 (8) (1997) 617.
39. G. Bereket, E. Hur, C. Ogretir, *J. Mol. Struct. Theochem.* 578 (2002) 79.
40. Gaussian 09, Revision B. 01, M. J. Frisch, G. W. Trucks, H. B. Schlegel, G. E. Scuseria, M. A. Robb, J. R. Cheeseman, G. Scalmani, V. Barone, B. Mennucci, G. A. Petersson, H. Nakatsuji, M. Caricato, X. Li, H. P. Hratchian, A. F. Izmaylov, J. Bloino, G. Zheng, J. L. Sonnenberg, M. Hada,

M. Ehara, K. Toyota, R. Fukuda, J. Hasegawa, M. Ishida, T. Nakajima, Y. Honda, O. Kitao, H. Nakai, T. Vreven, J. A. Montgomery, Jr., J. E. Peralta, F. Ogliaro, M. Bearpark, J. J. Heyd, E. Brothers, K. N. Kudin, V. N. Staroverov, T. Keith, R. Kobayashi, J. Normand, K. Raghavachari, A. Rendell, J. C. Burant, S. S. Iyengar, J. Tomasi, M. Cossi, N. Rega, J. M. Millam, M. Klene, J. E. Knox, J. B. Cross, V. Bakken, C. Adamo, J. Jaramillo, R. Gomperts, R. E. Stratmann, O. Yazyev, A. J. Austin, R. Cammi, C. Pomelli, J. W. Ochterski, R. L. Martin, K. Morokuma, V. G. Zakrzewski, G. A. Voth, P. Salvador, J. J. Dannenberg, S. Dapprich, A. D. Daniels, O. Farkas, J. B. Foresman, J. V. Ortiz, J. Cioslowski, and D. J. Fox, Gaussian, Inc., Wallingford CT, 2010.
41. A. Popova, *Corros. Sci*. 49 (2007) 2144.
42. A. Popova, E. Sokolova, S. Raicheva, M. Christov, *Corros. Sci*. 45 (2003) 33.
43. A. Popova, M. Christov, A. Vasilev, *Corros. Sci*. 49 (2007) 3276.
44. I.A. Ammar, F.M. El Khorafi, *Werk. Korro*. 24 (1973) 702.
45. T. Szauer, A. Brandt, *Electrochim. Acta* 26 (1981) 1209.
46. M A. Amin, M.A. Ahmed , H.A. Arida , T. Arslan d, M. Saracoglu and F. Kandemirli , *Corro. Sci.* 53 (2011) 540.
47. M. Elachouri, M.S. Hajji, M. Salem, S. Kertit, J. Aride, E. Essassi, *Corrosion* 52 (1996) 103.
48. L.B. Tang, G.N. Mu, G.H. Liu, *Corros. Sci*. 45 (2003) 2251.
49. G.N. Mu, X.M. Li, F. Li, *Mater. Chem. Phys*. 86 (2004) 59.
50. S.N. Banerjee, S. Misra, *Corrosion* 45 (1989) 780.
51. E.S. Ferreira, C. Giacomelli, F.C. Giacomelli, A. Spinelli, Mater. *Chem. Phys*. 83 (2004) 129.
52. S.S. Abd El-Rehim, H.H. Hassan, M.A. Amin, *Corros. Sci.* 46 (2004) 5-25.
53. F. Mansfeld, M.W. Kending, S. Tsai, *Corrosion* 37 (1981) 301-308.
54. A.P. Yadav, A. Nishikata, T. Tsuru, *Corros. Sci.* 46 (2004) 169-181.
55. A. Galal, N.F. Atta, M.H.S. Al-Hassan, *Mater. Chem. Phys.* 89 (2005) 38.
56. M.A. Ajmal, J. Rawat, M.A. Quarishi, *Br. Corros. J.* 24 (1999) 220.
57. K.F. Khaled, *Appl. Surf. Sci.* 252 (2006) 4120.
58. J.N. Murrell, S.F. Kettle, J.M. Tedder, The Chemical Bond, John Wiley & Sons, Chichester, 1985, 38.
59. C. Gruber, V. Buss, *Chemosphere* 19 (1989) 1595.
60. C.T. Wang, S.H. Chen, H.Y. Ma, C.S. Qi, *J. Appl. Electrochem*. 33 (2003)179-186.
61. D.F.V. Lewis, C. Ioannides, D.V. Parke, *Xenobiotica* 24 (1994) 401.
62. Z. Zhou, R.G. Parr, *J. Am. Chem. Soc.* 112 (1990) 5720.
63. R.G. Pearson, *Proc. Nat. Acad. Sci.* 83 (1986) 8440.
64. O. Kikuchi , *Quant. Struct.-Act. Relat.* 6 (1987) 179.
65. K.K. Khaled, K. Babic-Samardja, N. Hackerman, *J. Appl. Electrochem.* 34 (2004) 697.
66. A. Yurt, S. Ulutas, H. Dal, *Appl. Surf. Sci.* 253 (2006) 919.
67. R.R. Annand, R.M. Hurd, N. Hackerman, *J. Electrochem. Soc.* 112 (1965) 138.
68. B. Sathianandhan, K. Balahrishman, N. Subramyar, *Br. Corros. J.* 5 (1970) 270.
69. F. Zucchi, G. Trabanelli, G. Brunoro, *Corros. Sci.* 33 (1992) 1135.
70. F. Zucchi, G. Trabanelli, C. Monticelli, *Corros. Sci.* 38 (1996) 147.
71. M.A. Quraishi, R. Sardar, *J. Appl. Electrochem.* 33 (2003) 1163.
72. L.I. Antropov, E.M. Makushin, V.F. Panasenko, Inhibitors of Metal Corrosion (Russia), Technika, Kiev, 1981, p. 182.
73. S. Dyatkina, B. Damaskin, *Elektrokhimya* 22 (1986) 1283-1288.